A New Catalysis for Benzene Production from Acetylene under UHV Conditions: Sn/Pt(111) Surface Alloys

Chen Xu, John W. Peck, and Bruce E. Koel*

Contribution from the Department of Chemistry, University of Southern California, Los Angeles, California 90089-0482. *Received July 23, 1992*

Abstract: The adsorption and reaction of acetylene on Pt(111) and the p(2×2) and ($\sqrt{3}\times\sqrt{3}$)R30°Sn/Pt(111) surface alloys were investigated with low energy electron diffraction (LEED), temperature programmed desorption (TPD), and Auger electron spectroscopy (AES). The presence of Sn atoms at the surface of the p(2×2) and ($\sqrt{3}\times\sqrt{3}$)R30°Sn/Pt(111) surface alloys strongly suppressed the decomposition of acetylene (C_2D_2) to deuterium and adsorbed carbon. As a result, a new reaction path is opened on the Sn/Pt(111) surface alloys—*benzene formation*. Besides benzene desorption, we also observed butadiene desorption, which is obviously a C_4 product of a stable intermediate in benzene production. The ($\sqrt{3}\times\sqrt{3}$)R30°Sn/Pt(111) surface shows the highest activity and selectivity for the formation of benzene and butadiene. Following C_2D_2 adsorption on the Pt(111) surface at 110 K, LEED shows a faint (2×2) pattern. After saturation dosing of acetylene on the p(2×2)Sn/Pt(111) surface at 110 K we find a large increase in the (2×2) LEED pattern intensity. This implies that an acetylene (2×2) substructure also forms on the p(2×2)Sn/Pt(111) surface.

Introduction

The palladium-catalyzed cyclotrimerization of acetylene has attracted a lot of attention because of the measurable amount of benzene formation found even under ultra-high-vacuum (UHV) conditions. Lambert and co-workers[1-8] have led the way in investigations of this system. A general mechanism for this reaction has been established which involves a sequential process ($C_2 \rightarrow C_4 \rightarrow C_6$), without either C-H or C-C bond cleavage. The C_4 intermediate was first identified by DC beam experiments.[1] Further support comes indirectly from high resolution electron energy loss spectroscopy (HREELS) measurements of C_4H_4 species produced by dissociative chemisorption of $C_4H_4Cl_2$.[4]

In contrast to Pd, the transition metals in the same group, Ni and Pt, do not show any reactivity for the cyclotrimerization of acetylene under UHV conditions. The decomposition of acetylene to hydrogen and adsorbed carbon is the only reaction pathway observed. This is generally thought to be due to the higher reactivity of Pt and Ni compared to Pd. On a Pt(111) surface below 330 K, acetylene adsorbs in a μ_3-η^2 configuration by rehybridization of the carbon atoms to ~sp^2.[5] Between 330 and 400 K adsorbed acetylene disproportionates to an adsorbed bridging ethylidyne (CCH_3) and an unidentified residue, possibly C_2H, which decompose further to hydrogen and carbon with heating to 800 K.

Pt-Sn bimetallic catalysts are becoming increasingly important for catalytic reforming.[9-12] In one type of reaction in the reforming process, saturated hydrocarbons are converted to aromatic hydrocarbons as selectively as possible because of the high antiknock quality of aromatic hydrocarbons. Pt-Sn alloys may be formed under certain conditions on supported Pt-Sn bimetallic catalysts,[10] and these alloys may be responsible for the selective aromatization reactions. Recent investigations of organic molecule adsorption on Sn/Pt(111) surface alloys have shown that the alloys have a greatly reduced reactivity for hydrocarbon dehydrogenation on clean Pt(111).[13,14] Thus, we were attracted to explore acetylene adsorption and reaction on Sn/Pt(111) surface alloys. We find that the decomposition of acetylene is strongly suppressed with increasing presence of Sn at the surface. As a result, benzene formation is promoted. Benzene and butadiene desorption is observed under UHV conditions below 400 K.

Experimental Methods

The experiments were performed in a stainless steel UHV chamber. The system is equipped with instrumentation for Auger electron spectroscopy (AES) and low energy electron diffraction (LEED), a shielded UTI quadrupole mass spectrometer (QMS) for temperature programmed desorption (TPD), and a directed beam doser for making sticking coefficient measurements. The system base pressure is 6×10^{-11} Torr. TPD measurements were made using the QMS in line-of-sight with the sample surface and using a linear heating rate of 4-5 K/s. The Pt(111) crystal can be cooled down to 95 K using liquid nitrogen or resistively heated to 1200 K. The temperature was measured by a chromel-alumel thermocouple spotwelded to the side of the crystal.

The Pt(111) crystal was cleaned using the procedure found in ref. 15. The p(2×2)Sn/Pt(111) and p($\sqrt{3}\times\sqrt{3}$)R30°Sn/Pt(111) surface alloys were prepared by evaporating Sn on the clean Pt(111) surface and subsequently annealing them to 1000 K for 10 s. Depending upon the initial Sn coverage, the annealed surface exhibited a (2×2) or ($\sqrt{3}\times\sqrt{3}$)R30° LEED pattern. The structure for these patterns has been assigned to the (111) face of Pt_3Sn and a substitutional surface alloy of composition Pt_2Sn,[16] as shown in Figure 1. Angle-dependent low energy ion scattering spectroscopy (LEISS) measurements using 500-1000 eV Li^+ clearly show that surface alloys (rather than Sn adatoms) are produced and that Sn atoms are almost coplanar with the Pt atom at the surface; Sn only protrudes ~0.022 ± 0.005 nm above the surface.[17] This indicates a strong interaction between Sn and Pt atoms. Hereafter, we will denote these surfaces as the (2×2) or $\sqrt{3}$Sn/Pt(111) surface alloys.

Because of the carbon contamination resulting from each adsorption and TPD experiment and the strong affinity of oxygen for Sn, the Sn/Pt(111) surface alloys must be newly prepared for each experiment. Sn was removed easily by sputtering at 1000 K for 15 min. The sputtered surface was then heated at 800 K in 2×10^{-8} Torr of O_2 and annealed to 1200 K. The cleanliness was checked by AES.

Acetylene (C_2D_2) was used as received from Cambridge Isotope Laboratories (CIL) and the purity was checked by in situ mass spectrometry. The sticking coefficient of acetylene was determined using a simple kinetic uptake method which was described previously.[18] The

(1) Tysoe, W. T.; Nyberg, G. L.; Lambert, R. M. *Surf. Sci.* **1983**, *135*, 128.
(2) Patterson, C. H.; Lambert, R. M. *J. Phys. Chem.* **1988**, *92*, 1266.
(3) Patterson, C. H.; Lambert, R. M. *J. Am. Chem. Soc.* **1988**, *110*, 6871.
(4) Patterson, C. H.; Mundenar, J. M.; Timbrell, P. Y.; Gellman, A. J.; Lambert, R. M. *Surf. Sci.* **1989**, *208*, 93.
(5) Ormerod, R. M.; Lambert, R. M. *J. Chem. Soc., Chem. Commun.* **1990**, 1421.
(6) Hoffman, H.; Zaera, F.; Ormerod, R. M.; Lambert, R. M.; Wang, L. P.; Tysoe, W. T. *Surf. Sci.* **1990**, *232*, 259.
(7) Ormerod, R. M.; Baddeley, C. J.; Lambert, R. M. *Surf. Sci.* **1991**, *259*, L709.
(8) Hoffman, H.; Zaera, F.; Ormerod, R. M.; Lambert, R. M.; Yao, J. M.; Saldin, D. K.; Wang, L. P.; Bennett, D. W.; Tysoe, W. T. *Surf. Sci.* **1992**, *268*, 1.
(9) Sinfelt, J. H. *Bimetallic Catalysis: Discoveries, Concepts, and Applications*; Wiley: New York, 1983; pp 130-157.
(10) Meitzner, G.; Via, G. H.; Lytle, F. W.; Fung, S. C.; Sinfelt, J. H. *J. Phys. Chem.* **1988**, *92*, 2925.
(11) Srinivasan R.; Rice, L. A.; Davis, B. H. *J. Catal.* **1991**, *129*, 257.
(12) Balakrishnan, K.; Schwank, J. *J. Catal.* **1991**, *132*, 451.
(13) Paffett, M. T.; Gebhard, S. C.; Windham, R. G.; Koel, B. E. *Surf. Sci.* **1989**, *223*, 449.
(14) Xu, C.; Koel, B. E. to be submitted for publication.
(15) Campbell, C. T.; Ertl, G.; Kuipers, H.; Segner, J. *Surf. Sci.* **1981**, *107*, 220.
(16) Paffett, M. T.; Windham, R. G. *Surf. Sci.* **1989**, *208*, 34.
(17) Overbury, S. H.; Mullins, D. R.; Paffett, M. T.; Koel, B. E. *Surf. Sci.* **1991**, *254*, 45.
(18) Jiang, L. Q.; Koel, B. E.; Falconer, J. L. *Surf. Sci.* **1992**, *273*, 273.

0002-7863/93/1515-751$04.00/0

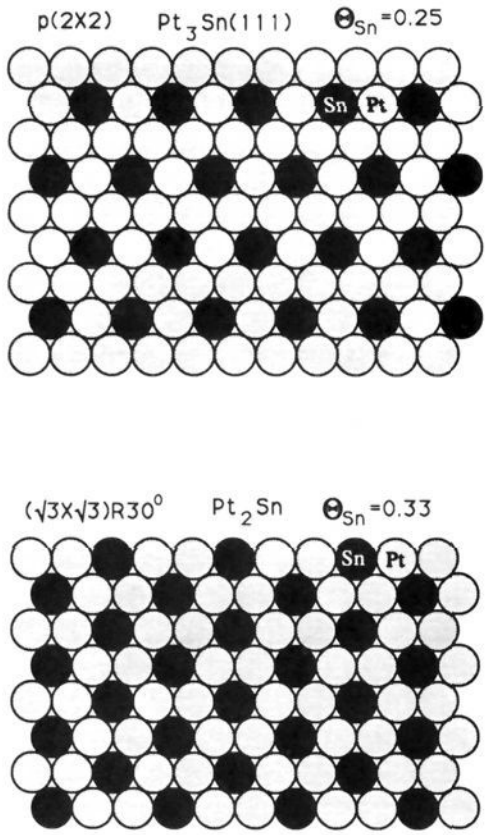

Figure 1. Structures for the (2×2) and (√3×√3)R30° Sn/Pt(111) surface alloys.

acetylene coverage, θ, was calibrated with the following equation,[19] using the well-known saturation coverage of CO, $\theta_{CO} = 0.5$,[15] on clean Pt(111) at 300 K:

$$\theta_{acetylene} = \frac{P_{acetylene}}{P_{CO}}\left(\frac{M_{CO}}{M_{acetylene}}\right)^{1/2}\frac{\int S_{acetylene}\,dt}{\int S_{CO}\,dt}\theta_{CO} \qquad (1)$$

Adsorbate coverages in this paper are referenced to the Pt(111) surface atom density, i.e., $\theta = 1$ is defined as 1.505×10^{15} cm^{-2}.

Results and Discussion

Acetylene Adsorption. The thermal desorption spectra of molecular acetylene and D_2 evolution after the Pt(111) and Sn/Pt(111) surface alloys are saturated with acetylene are summarized in Figures 2 and 3. The TPD spectra from clean Pt(111) are in good agreement with data published previously.[20-22] Using the TPD area we estimate that molecular C_2D_2 desorption is less than 2% of the amount of adsorbed acetylene. Hence C_2D_2 adsorption is largely irreversible. This is also consistent with previous studies.[20-22]

Increasing the amount of Sn in the alloy strongly increases the amount of molecular acetylene desorption. For the (2×2) surface alloy, we see three molecular acetylene peaks between 300 and 550 K. On the √3 surface alloy, the TPD spectra of acetylene is dominated by a large peak at 365 K. Since we use C_2D_2, which has the same mass as CO, it is reasonable to ask about the CO contribution to the TPD spectra. In order to check out the possible CO contribution, we also monitored the intensity of mass 26 which is a cracking product of acetylene. Both the relative peak intensities and the desorption peak temperatures of mass 26 are identical with those of mass 28. These results indicate a negligible CO contribution to the C_2D_2 TPD spectra.

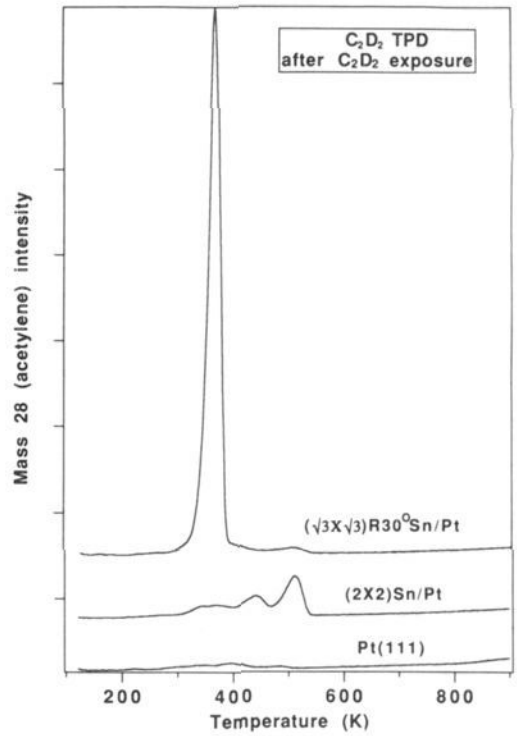

Figure 2. C_2D_2 TPD spectra after acetylene saturation exposure on the Pt(111) surface (bottom curve), (2×2)Sn/Pt(111) surface alloy (middle curve), and (√3×√3)R30°Sn/Pt(111) surface alloy (top curve) at 110 K.

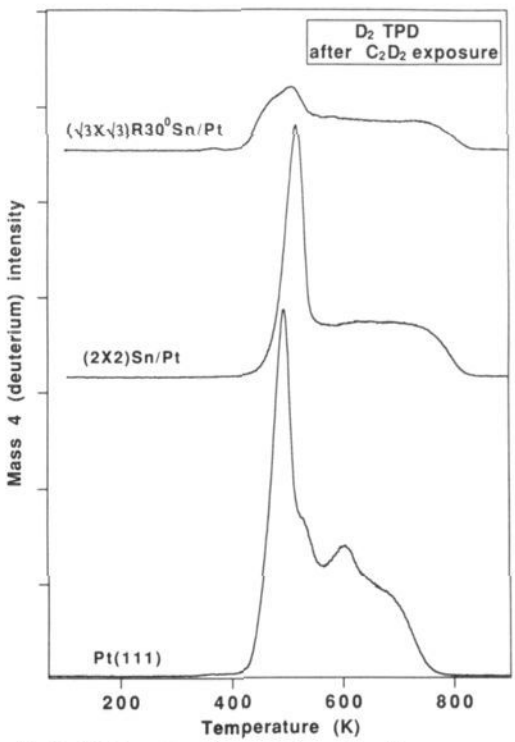

Figure 3. D_2 TPD spectra after acetylene saturation exposure on the Pt(111) surface (bottom curve), (2×2)Sn/Pt(111) surface alloy (middle curve), and (√3×√3)R30°Sn/Pt(111) surface alloy (top curve) 110 K.

D_2 evolution from C_2D_2 decomposition is strongly suppressed by adding Sn to the Pt(111) surface. But we still have marked amounts of D_2 desorption on both Sn/Pt(111) surface alloys. Even on the √3 surface alloy more than 35% of the adsorbed acetylene decomposed, as estimated from the D_2 TPD area. With increasing Sn presence on the surface, the D_2 desorption temperature also

(19) Jiang, L. Q.; Koel, B. E. *J. Phys. Chem.* **1992**, *96*, 8694.
(20) Megiris, C. E.; Berlowitz, P.; Butt, J. B.; Kung, H. H. *Surf. Sci.* **1985**, *159*, 184.
(21) Abon, M.; Billy, J.; Bertolini, J. C. *Surf. Sci.* **1986**, *171*, L387.
(22) Avery, N. R. *Langmuir* **1988**, *4*, 445.

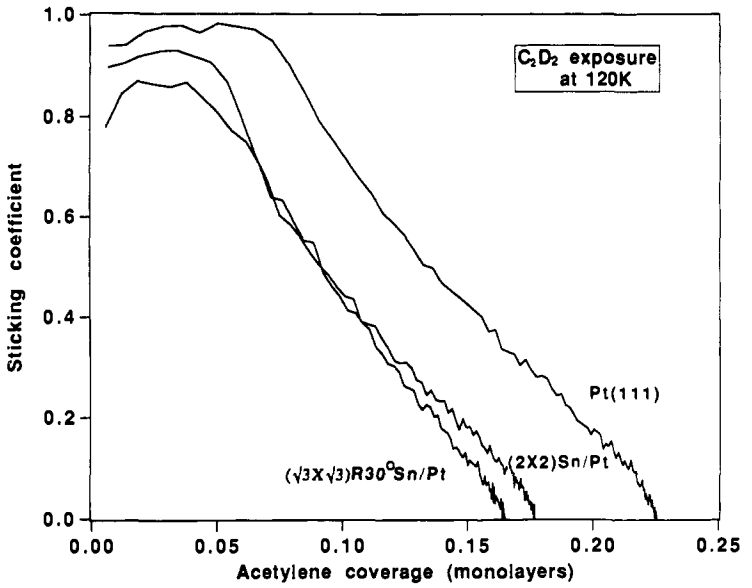

Figure 4. Sticking coefficient of acetylene on the Pt(111) surface, (2×2)Sn/Pt(111) surface alloy, and (√3×√3)R30°Sn/Pt(111) surface alloy at 120 K.

changes. The peak at 495 K shifts to 515 K and the peaks between 500 and 800 K are replaced by a structureless, broad peak upon changing from the clean Pt(111) surface to the (2×2) surface alloy. Increasing further the amount of Sn in the alloy to form the √3 surface alloy does not change the desorption temperature of the sharp peak at 515 K. But the size of this peak decreases sharply, and it is accompanied by a new, broad peak around 490 K.

H_2 adsorption and desorption on Pt(111) and the (2×2) and √3 surface alloys has been studied by Paffett et al.[23] On all three surfaces, the highest desorption peak is around 400 K. Therefore, the desorption kinetics of all D_2 TPD peaks from acetylene decomposition are reaction rate-limited by C–H bond breaking reactions on the surface. The change from clean Pt(111) to the (2×2) surface alloy indicates an increase in the activation energy of C–H bond cleavage which might be caused by site-blocking effects, although we certainly cannot exclude electronic effects on this change.

In Figure 3, the higher temperature tail of the D_2 TPD spectra shifts to higher temperature by almost 50 K from the Pt(111) surface to the Sn/Pt(111) surface alloys. This change indicates a large increase in the activation energy for the C–H bond cleavage involved in the complete dehydrogenation of hydrocarbon species remaining on the surface at very high temperatures.

The results of C_2D_2 sticking coefficient measurements on the three surfaces at 120 K are summarized in Figure 4. The initial sticking coefficient, evaluated in the limit of zero C_2D_2 coverage, is near unity on the Pt(111) surface and also very large (>0.8) on the two alloys. The sticking coefficients on all three surfaces are constant out to about 25% of the saturation coverage and then decrease gradually to zero at saturation coverage. These results indicate the important role of a mobile precursor, i.e., transient, adsorbed species, in the adsorption kinetics on all three surfaces. With increasing Sn concentration in the surface, both the sticking coefficients and the saturation coverages decrease slightly. The saturation coverage on both Sn/Pt(111) surface alloys is reduced by around 20–25% with respect to the clean surface. For a proper picture of the reaction kinetics on heterogeneous catalysts, in particular supported, bimetallic Pt–Sn catalysts, it is also important to mention that both the initial sticking coefficient and the saturation coverage of acetylene are not simple functions of the Sn concentration on the surface as one might expect from simple site-blocking arguments. These data should also resolve a controversy over the saturation coverage of acetylene on the clean Pt(111) surface. It has been proposed to be either 0.25 monolayer[21] or 0.5 monolayer.[24] Our result strongly supports 0.25 monolayer.

The adsorption of acetylene on the two Sn/Pt(111) surface alloys was also investigated with LEED. Dosing acetylene on clean Pt(111) at 110 K caused no additional LEED pattern. Heating the sample to 300 K after a saturation dose at 110 K formed a diffuse (2×2) LEED pattern. This result is consistent with the data reported by Stair and Somorjai.[25] They observed a diffuse (2×2) LEED pattern after dosing small amounts of acetylene at 300 K. Further dosing of acetylene to saturation coverage destroyed the (2×2) LEED pattern. This difference between the low temperature and room temperature dosing is consistent with the finding that the saturation coverage of acetylene at 300 K is 40% higher than the saturation coverage at 120 K.[21] The change in saturation coverage at different temperatures can be explained as a change of adsorption geometry, from a side-bonded acetylene at 120 K to an upright species at 300 K. The species at 300 K wa first identified as vinylidene,[26–28] but this assignment has been questioned by the more recent HREELS studies of Avery[22] who has reassigned this species to ethylidyne.

Dosing a saturation coverage of acetylene on the (2×2) surface alloy at 110 K strongly increases the intensity of the fractional order spots in the (2×2) LEED pattern strongly. These spots become as sharp and intense as the first-order spots in the (1×1) pattern. Upon heating the sample, the (2×2) LEED pattern again loses intensity at around 520 K. This correlates to the first large D_2 evolution peak. Both the increase in the LEED pattern intensity after dosing acetylene at 110 K and the decrease in the intensity after heating to 520 K are reproducible. We believe that acetylene also forms a (2×2) ordered structure on the (2×2)-Sn/Pt(111) surface alloy. Dosing acetylene on the √3 surface alloy causes neither any additional LEED pattern nor an increase in the intensity of the fractional-order spots in the original LEED pattern and so adsorbed acetylene is disordered on this surface.

Benzene Formation. The cyclotrimerization of acetylene to form benzene was also monitored with TPD. The results are summarized in Figure 5. Figure 5a provides TPD spectra of benzene formation on clean Pt(111) and the (2×2) and √3 surface alloys. After saturation of clean Pt(111) with acetylene, only a tiny benzene desorption peak is seen. Alloying with Sn strongly

(23) Paffett, M. T.; Gebhard, S. C.; Windham, R. G.; Koel, B. E. *J. Phys. Chem.* **1990**, *94*, 6831.

(24) Freyer, N.; Pirug, G.; Bonzel, H. P. *Surf. Sci.* **1983**, *126*, 487.
(25) Stair, P. C.; Somorjai, G. A. *J. Chem. Phys.* **1977**, *66*, 2036.
(26) Ibach, H.; Lehwald, S. *J. Vac. Sci. Technol.* **1978**, *15*, 407.
(27) Demuth, J. E. *Surf. Sci.* **1979**, *80*, 367.
(28) Wang, P. K.; Slichter, C. P.; Sinfelt, J. H. *Phys. Rev. Lett.* **1984**, *53*, 82.

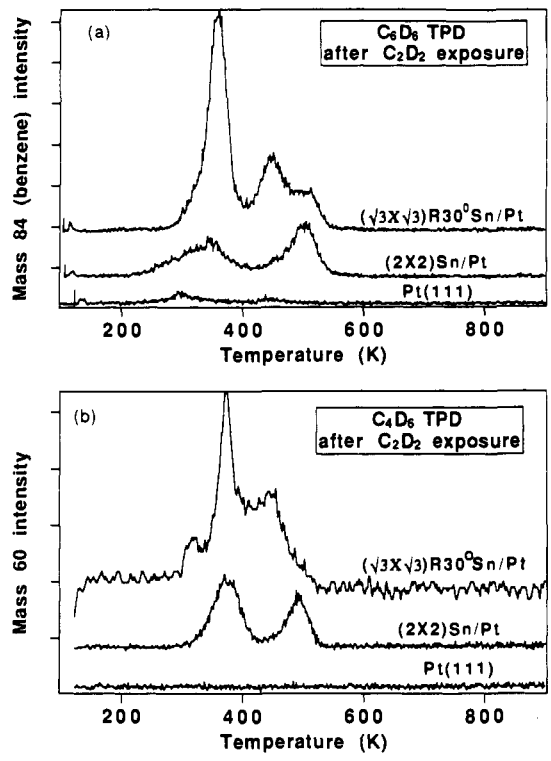

Figure 5. (a) C_6D_6 and (b) C_4D_6 TPD spectra after acetylene saturation exposure on the Pt(111) surface, (2×2)Sn/Pt(111) surface alloy, and (√3×√3)R30°Sn/Pt(111) surface alloy at 110 K.

promotes benzene formation as is indicated by the large increase in the benzene TPD peak. The case for benzene formation is supported by other mass spectral data. In addition to mass 84, we also monitored masses 54 and 82, the major cracking fractions of benzene. The TPD spectra of masses 54 and 82 identically follow the shape of the TPD spectra at mass 84.

We also monitored the formation and desorption of possible intermediate products. The TPD spectra for C_4D_6 desorption are shown in Figure 5b. On clean Pt(111), no C_4D_6 desorption is seen. The evolution of C_4D_6, butadiene, is strongly promoted with increasing Sn concentration in the surface. Besides mass 60 for butadiene, we also monitored masses 42 and 58, two main cracking products of butadiene. The TPD spectra (not shown) of mass 42 and 58 follow the same shape of the TPD spectra for mass 60. These results support our assignment of butadiene desorption. Furthermore, the relative intensity of these three masses suggests a 1,3-butadiene species. It is interesting to mention at this point that the addition of two acetylene molecules only produces an adsorbed C_4D_4 species which is not stable in the gas phase. In order to produce butadiene, two additional hydrogens must be attached. Since we would expect this process to have a small rate constant, we might have a relatively large C_4D_4 concentration on the surface at some temperature prior to C_4D_6 desorption.

In order to get some insight into the mechanism of the cyclotrimerization reaction, we compare three different TPD spectra on the √3 surface alloy in Figure 6. Molecular acetylene desorption after a saturation acetylene dose is shown in Figure 6a. A TPD spectrum of benzene formation from this acetylene dose is shown in Figure 6b. A benzene TPD spectrum after dosing benzene to the surface is also provided in Figure 6c. It is easy to recognize from Figure 6 that the desorption temperature of benzene formed from acetylene is much higher than that of directly dosed benzene. This indicates that the desorption of benzene formed from acetylene is not limited by the benzene desorption rate but is a reaction rate limited process. The first desorption peak at 350 K in Figure 6b is 50 K higher than that of directly dosed benzene, but 15 K lower than the desorption temperature of acetylene.

Our proposed mechanism for acetylene cyclotrimerization is as follows. Acetylene adsorbs at low temperatures as individual

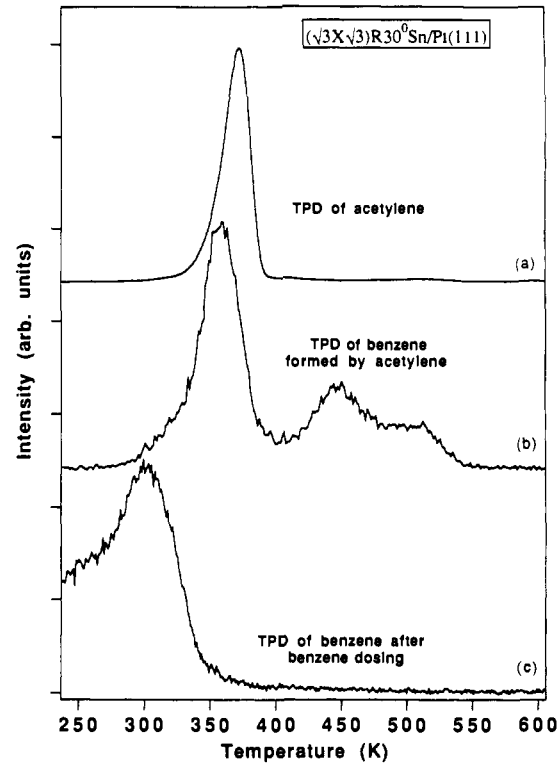

Figure 6. Comparison of TPD spectra of (a) C_2D_2 and (b) C_6D_6 after acetylene saturation exposure at 110 K and (c) TPD spectrum of C_6H_6 after C_6H_6 dosing on the (√3×√3)R30°Sn/Pt(111) surface alloy at 110 K.

molecules on the √3 surface alloy. The interactions between the molecules are small. Around 300 K, some adsorbed hydrocarbon intermediate is formed on the surface. This temperature is also suggested for the cyclotrimerization reaction of acetylene on the Pd(111) surface.[4] Because of the newly formed C–C bonds, the bonding of the intermediate to the surface is weakened compared to acetylene. Upon further heating to 350 K, 15 K lower than the acetylene desorption temperature, this intermediate species desorbs from the surface as butadiene. The hydrogen comes from disproportionation or decomposition of either adsorbed acetylene or the adsorbed C_4 intermediate. Benzene formation at the same temperature is detected by TPD. After desorbing much of the acetylene at 365 K, only ≃40% of the surface is covered by hydrocarbons from previously adsorbed acetylene. Further heating liberates additional hydrogen from the adsorbates, driving additional reactions and condensation, and causes benzene formation again at 450 and 500 K.

An alternative explanation which can account for the 15 K lower desorption temperature of butadiene than acetylene is that the C_4 intermediate formation/hydrogenation is the rate-limiting process for observation of butadiene, rather than butadiene desorption. So, competition between acetylene dimerization and desorption may cause butadiene to desorb at a lower temperature than acetylene as opposed to weaker bonding to the surface by the C_4 intermediate.

Using the C_6D_6 TPD area and the known saturation coverage of 0.03 monolayers from directly dosed benzene on the √3 surface alloy in sticking coefficient measurements (benzene exposed on the √3 surface alloy does not decompose[14]), we can estimate the amount of benzene formed by acetylene cyclotrimerization to be about 10% of the acetylene saturation coverage on the √3 surface alloy, which is 0.16 monolayer.

Previously, the formation of benzene from acetylene has only been observed under UHV conditions on Pd[1-8] and Cu[29] surfaces. A definitive reason for the absence of this reaction on Pt surfaces has not been advanced. With the alloying of Sn on a Pt(111)

(29) Avery, N. Y. *J. Am. Chem. Soc.* **1985**, *107*, 6711.

surface we have been able to stimulate the formation of benzene from an acetylene adlayer. It is possible that through further examination of this model system we might be able to discover which of platinum's properties normally prohibit the formation of benzene from acetylene, and how the presence of Sn in the surface alloy alters the Pt surface so that the reaction can take place. In a separate experiment we have found that carbon, which usually acts as a site blocker, cannot promote benzene formation.[30] Therefore, an electronic effect of Sn must be important in the production of benzene.

Acknowledgment. This work was supported by the U.S. Department of Energy, Office of Basic Energy Sciences, Chemical Sciences Division.

(30) Peck, J. W.; Xu, C.; Koel, B. E., to be submitted for publication.

Comments Concerning the Computation of ^{113}Cd Chemical Shifts

Paul D. Ellis,* Jerome D. Odom,* Andrew S. Lipton, and James M. Gulick

Contribution from the Department of Chemistry and Biochemistry, University of South Carolina, Columbia, South Carolina 29208. *Received February 28, 1992*

Abstract: We have examined the ^{113}Cd chemical shift difference between dimethyl- and diethylcadmium from both an experimental and a theoretical perspective. Further, we have determined the chemical shift difference in the gas phase, in which diethylcadmium is more shielded than dimethylcadmium by 142.6 ppm. In contrast to other reported calculations, we demonstrate that these chemical shifts cannot be calculated quantitatively. The reasons for this lack of quantitation are discussed.

In the past several years, we[1] and others[2] have developed and utilized Cd^{2+} via ^{113}Cd NMR spectroscopy as a "spin-spy" to study Zn^{2+} and Ca^{2+} sites in metal-dependent proteins and metalloproteins. The reasoning behind this strategy is the fact that Zn^{2+} and Ca^{2+} have such poor spectroscopic properties. Both have closed shell electron configurations; hence, ESR spectroscopy is unavailable. Further, both have d^{10} electron configurations; therefore, their UV/vis spectroscopy lacks "color" and distinction. As a consequence of these "boring" spectroscopic properties, other alternatives have been pursued, i.e., the surrogate probe strategy as a means to study these metals in this important class of biological systems. In every case studied to date, the surrogate strategy has been successful, i.e., it has provided results which are consistent with the known chemistry of the system of interest. ^{113}Cd NMR spectroscopy is recognized as one of the best (if not the best) spectroscopic methods with which to understand the ligand chemistry and dynamics associated with Zn^{2+} or Ca^{2+} sites in metalloproteins.[2] Parallel to these efforts are fundamental experiments directed toward the understanding of the structural and electronic basis for these metal ion magnetic resonance parameters, e.g., chemical shifts and shielding tensors. Single crystal NMR experiments[1d-f] have been utilized to correlate X-ray data with these tensor quantities. With such correlations, empirical models[1g] have been developed that can be utilized to predict the orientation of shielding tensors of metal ions. Similar models can be developed for electric field gradient tensors. These models form the basis for the understanding of the protein-metal ion shielding data.[1c] These models also have the advantage that they can be tested by ab initio MO methods for calculating shielding tensors.

We have been interested in the calculation of shielding tensors[3] for several years. However, only recently have we begun to perform calculations of ^{113}Cd shielding tensors via ab initio MO methods. The reason for this delay has been 2-fold. First, we believe that these shielding tensors have significant relativistic contributions from L·S terms, and second, the importance of the contribution that electron correlation makes to these shielding tensors is unknown. The spin-orbit terms arise from the uncoupling of the angular momentum and spin by the applied magnetic field. The basis for this hypothesis is the position of cadmium in the periodic table. As is well known from atomic spectroscopy, l and m_s are no longer good quantum numbers for elements with atomic number greater than approximately 35 (Br) to 40 (Zr).[4] Further, for electron velocities Hartree[5] states, "For an atom of atomic number N, velocities (in atomic units) are on the order of N^2; so relativistic effects are of order $(N/137)$." For cadmium, N is 48 and $(N/137)^2$ is 0.123. For other metal ions of biological interest, e.g., Zn, Mo, and Hg, $(N/137)^2$ is 0.048, 0.094, and 0.341, respectively. Relativistic effects should be noticeable for cadmium and especially mercury. Cadmium and mercury are known[6] to have parallel trends in shielding, with an increased sensitivity for mercury.

Given this perspective, we were surprised to read a paper by Nakatsuji and co-workers[7] which stated that ^{113}Cd chemical shifts could be calculated quantitatively by ab initio coupled Hartree-Fock (CHF) methods. The experimental systems treated were organocadmium compounds, i.e., dimethylcadmium, diethylcadmium, and ethylmethylcadmium. The chemical shift difference for dimethyl- and diethylcadmium, 99.7 ppm for the neat liquids, was difficult for us to explain in our original determination.[1a] We noted in that work that a chemical shift difference may result from self-association in the neat liquids.

The results of Nakatsuji and co-workers[7] looked excellent; however, on closer examination some puzzling questions arose.

(1) (a) Cardin, A. D.; Ellis, P. D.; Odom, J. D.; Howard, J. W. *J. Am. Chem. Soc.* **1975**, *97*, 1672. (b) Ellis, P. D. *Science* **1983**, *221*, 1141. (c) Ellis, P. D. *J. Biol. Chem.* **1989**, *264*, 3108. (d) Rivera, E.; Kennedy, M. A.; Adams, R. D.; Ellis, P. D. *J. Am. Chem. Soc.* **1990**, *112*, 1400. (e) Rivera, E.; Kennedy, M. A.; Ellis, P. D. *Adv Magn. Reson.* **1989**, *13*, 257. (f) Marchetti, P. S.; Honkonen, R. S.; Ellis, P. D. *J. Magn. Reson.* **1987**, *71*, 294. (g) Honkonen, R. S.; Ellis, P. D. *J. Am. Chem. Soc.* **1984**, *106*, 5488. (h) Marchetti, P. S.; Ellis, P. D.; Bryant, R. G. *J. Am. Chem. Soc.* **1985**, *107*, 8191.

(2) Summers, M. F. *Coord. Chem. Rev.* **1988**, *86*, 43.

(3) Ditchfield, R.; Ellis, P. D. In *Topics in Carbon-13 NMR Spectroscopy* Vol. 1; Levy, G. C.; Ed.; Wiley and Sons: New York, 1974; 1-51.

(4) Slater, J. C. *Quantum Theory of Atomic Structure*; McGraw-Hill: New York, 1960. Shu, F. H. *The Physics of Astrophysics*; University Science Books: Mill Valley, California, 1991; 302. Karplus, M.; Porter, R. N. *Atoms & Molecules: An Introduction For Students of Physical Chemistry*; W. A. Benjamin, Inc.: New York, 1970; 210.

(5) Hartree, D. R. *The Calculation of Atomic Structures*; Wiley and Sons: New York, 1957.

(6) A recent example is in: Santos, R. A.; Gruff, E. S.; Koch, S. A.; Harbison, G. S. *J. Am. Chem. Soc.* **1990**, *112*, 9257.

(7) Nakatsuji, H.; Nakao, T.; Kanda, K. *Chem. Phys.* **1987**, *118*, 25.

0002-7863/93/1515-755$04.00/0